THE JOURNAL OF PHYSICAL CHEMISTRY A LETTERS

2005, *109,* 4979−4982
Published on Web 05/18/2005

Broken Inter-C_{60} Bonds as the Cause of Magnetism in Polymeric C_{60}: A Density Functional Study Using C_{60} Dimers

Jordi Ribas-Ariño,[†] Alessandro Curioni,[‡] Wanda Andreoni,[‡] and Juan J. Novoa*,[†,§]

Departament de Química Física, Facultat de Química, and CERQT, Parc Científic, Universitat de Barcelona, Av. Diagonal 647, 08028-Barcelona, Spain, IBM Research, Zurich Research Laboratory, 8803 Rüschlikon, Switzerland, and CEPBA-IBM Research Institute

Received: February 11, 2005; In Final Form: May 3, 2005

Bond breaking in $C_{60}-C_{60}$ dimeric units is believed to play an important role in the onset of magnetism in 2D polymeric C_{60}. On the basis of density-functional theory, the calculations we present here provide further insight into this mechanism through a quantitative characterization of the bond-breaking processes in the isolated dumbbell-shaped C_{60} dimer. In particular, the analysis of the calculated potential energy surfaces for the low-lying singlet and triplet states identifies and locates the S_0-T_2 crossing point, which is crucial for the transition to a magnetic state to take place under thermal conditions. These results also suggest a possible new approach to the production of magnetic polymeric C_{60}.

Since the discovery of ferromagnetic behavior in 2D rhombohedral polymeric C_{60} under high-pressure and high-temperature conditions,[1] a number of diverse experiments have been performed that provide solid support for such an unexpected observation.[2−7] In particular, experimental evidence has been produced that indicates that magnetism is an intrinsic property of pristine C_{60} in this phase: it is not induced by impurities,[2,3,6] and the radical centers responsible for it form without damaging the C_{60} cage.[7]

Despite several attempts to explain the onset and subsequent establishment of magnetic order, a complete understanding of its physical origin still requires further progress. A few contrasting models have been proposed to describe the mechanism generating the radical centers (e.g., the presence of structural defects such as atomic vacancies[8] or open-cage C_{60} isomers[9,10] and the partial breaking of intermolecular bonds, leading to states of higher spin multiplicity[11,12]). In particular, two of us[11] have recently reported ab initio calculations of the C_{60} dimer, described using an approximate structural model, which is the smallest and most convenient system to use in studying the bonding in polymeric C_{60} solids. It was pointed out that under shortening of the intermolecular distance from equilibrium one of the two intermolecular bonds tends to break and that the character of the ground state simultaneously changes from singlet (S_0) to triplet (T_2). This naturally led to an appealing proposal for the mechanism responsible for the onset of magnetism in the condensed phase. However, now another step forward is mandatory, namely, the identification of the hypothesized[11] crossing between the S_0 and T_2 potential energy surfaces, which is the necessary condition for the rupture to take place in thermally triggered processes. Locating such a crossing and estimating the energy profile of the transition are the scope of the investigation we present in this letter. Specifically, density-functional theory (DFT)[13] calculations were performed to explore the most relevant regions of the potential energy surfaces (PES) of the S_0, T_1, and T_2 electronic states of the dumbbell C_{60} dimer,[14] their stationary points, and the energy barriers for dimerization. Our results allow us to speculate on a possible scenario for the propagation of the excitation and also lead to suggestions for new methods to produce these magnetic nanostructures.

The DFT calculations we describe below were performed in the pseudopotential-plane-waves framework of the CPMD code[15] using the BLYP[16] approximation for the exchange-correlation functional, norm-conserving *l*-dependent pseudopotentials,[17] and a cutoff of 55 Ry for the plane-wave expansion.[18] This computational scheme has been extensively applied to the study of chemical and physical properties of fullerenes and fullerene derivatives.[19] We also report on some results obtained in the all-electron scheme of the Gaussian 98 code[20] using different local Gaussian basis sets and the hybrid B3LYP [21] prescription for the exchange-correlation functional. Clearly these are intended to give us an idea regarding the dependence (if any) of the results on the specific DFT implementation. The broken-symmetry approach[22] was used to describe the singlet wave function in regions of the potential energy surface where the singlet wave functions are open-shell in nature (whenever bonds are partially or fully broken). The quality of the broken-symmetry DFT approach was tested: an extensive calculation of the PES of the S_0 electronic state of two ethylene molecules (made within the B3LYP/3-21G scheme) showed that the shape and main features of the PES calculated with the DFT methods are similar to those obtained with the multiconfiguration CASSCF method[23] using the same basis set.[24] They also allowed us to identify the most relevant regions of the PES to be investigated for the larger dimer.

* Corresponding author. E-mail: juan.novoa@ub.edu.
† Universitat de Barcelona.
‡ IBM Research.
§ CEPBA-IBM Research Institute (associate member).

10.1021/jp050753d CCC: $30.25

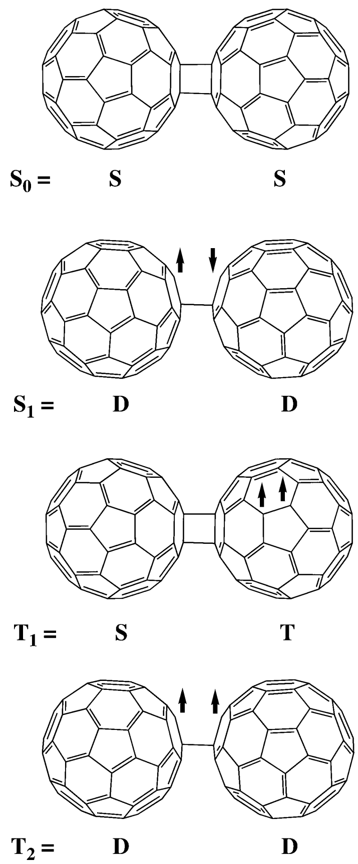

Figure 1. Structure of the S_0, S_1, T_1, and T_2 states.

Experimentally, the dumbbell-shaped C_{60} dimers result from a [2 + 2] cycloaddition of two C_{60} molecules when either light or pressure is applied to pristine C_{60} crystals.[25,26] Depending on the experimental conditions, multiple [2 + 2] cycloadditions may also take place, giving rise to either 1D chains or 2D polymers.[27] (So far, no 3D cases have been found.) In each of these cycloadditions, two new intermolecular C−C bonds are formed that connect the carbon atoms at the fusion of the six-membered rings ([6:6]) on each fragment. This configuration corresponds to the S_0 singlet ground state depicted in Figure 1. Studying the lowest T_1 and T_2 triplet states (Figure 1) is critical for the present study. Indeed, one can think of T_1 and T_2 as having been generated from the S_0 state after breaking one "double" bond in one of the C_{60} cages (such that the two electrons are left in a triplet configuration) and one of the two intermolecular bonds, respectively. They are different triplet states (Figure 2); whereas in T_2 each C_{60} unit holds one spin, experimental studies[28] showed that in T_1 the spin density is distributed over only one of two C_{60} molecules, localized on opposite atoms along the equator (a distribution also found in the triplet state of C_{60} fullerenes[29]). Also, the lowest singlet excited state (S_1) (Figure 1) can be thought of as resulting from the homolytic rupture of one interfragment C−C bond as for the T_2 state, to which it is closely related. We found that the PESs of the S_1 and S_0 states are interconnected, by analogy to the scenario described by CASSCF calculations for the ethylene dimer.[23] From now on, we will refer to the lowest-energy singlet PES as S_0, although one has to keep in mind that the electronic structure evolves from S_0 to S_1 when the interfragment C−C distance is elongated.

After determining the configuration corresponding to the global energy minimum for each state, calculations proceeded by progressively changing the interfragment C−C distance. In

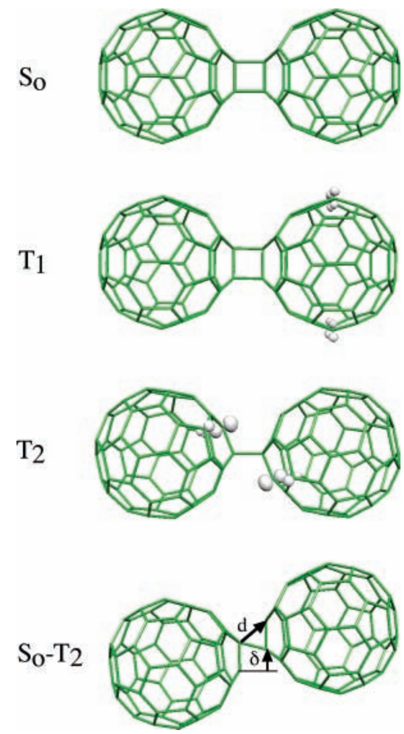

Figure 2. Geometry of the minimum-energy configurations of the S_0, T_1, and T_2 states. (In T_1 and T_2, the distribution of a spin density isosurface is also depicted.) Also represented is the geometry of the configuration of lowest energy where the S_0 and T_2 surfaces cross. (d and δ are the parameters that quantify the parallel drift motion of one C_{60} fragment with respect to the other.)

TABLE 1: C_{60} Dimer: Main Characteristics of the PES of the S_0, T_1, and T_2 Lowest Electronic States[a]

state	E_{min}	d	*d* [6:6]	*E**(exp)	*E**(theory; this work)	*E**(theory[b])	E_F
S_0	0	1.616	1.614	29[c], 30[d]	29 (sy)	44 (sy)	27
					28 (asy)	37 (asy)	
T_1	28.5[e]	1.605	1.605	15[d]	13 (sy)		21[f]
T_2	19	1.709	1.526		5 (asy)		11[f]

[a] For each state, E_{min}, *d*, and *d*[6:6] are the energy relative to the S_0 minimum, the interfragment C−C distance, and the [6:6] intrafragment distance (Figures 1 and 2) calculated for the optimized structure; *E** is the dissociation barrier; and E_F is the formation energy with respect to the two separate C_{60} monomers in the appropriate state. (See the text.) All energies are in kcal/mol, and all distances, in Å. [b] Porezag et al. in ref 14. [c] Wang, Y.; Holden, J. H.; Bi, X.; Eklund, P. C. *Chem. Phys. Lett.* **1993**, *217*, 3. [d] Reference 28a. [e] Experimental estimate is 34 kcal/mol (ref 28a). [f] The calculated energy of the lowest triplet state for the monomer is 35 kcal/mol above the singlet ground state.

Table 1, we report information on the properties of these states and some characteristics of the PES that we calculated and compare our results with those of previous calculations and especially with available experimental data. Moreover, a convenient representation of the PES is shown in Figure 3, which illustrates the potential energy curves for synchronous (S_0 and T_1) and asynchronous (T_2) approaches of the two C_{60} molecules as a function of the shortest interfragment C−C distance (shown as solid lines that connect the C_{60} units in Figure 1). Asynchronous curves corresponding to the S_0 and T_1 states have also been computed but are not plotted here, for the sake of clarity. Each point on these curves corresponds to a global optimization of the atomic coordinates under the constraint of a fixed value for the interfragment C−C distance. In the synchronous curves, the two interfragment C−C distances are forced to be the same length and the rest of the geometrical

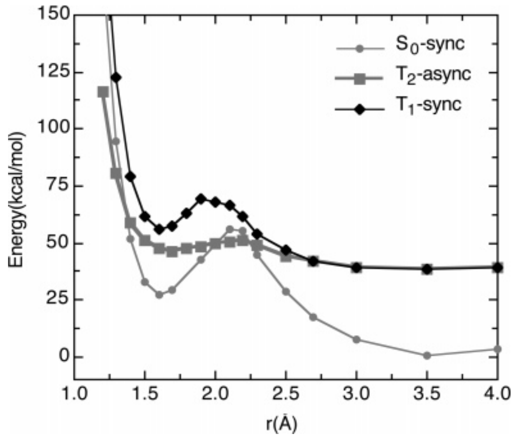

Figure 3. Potential energy curves for the dissociation of the dumbbell $C_{60}-C_{60}$ dimer into two C_{60} fragments. The zero of energy corresponds to two isolated C_{60} molecules in their singlet ground state.

parameters are fully optimized, whereas in the asynchronous curves only one interfragment C−C distance is fixed and the other is optimized together with the remaining geometrical parameters. The S_0, T_1, and T_2 states exhibit an energy minimum and an energy barrier towards the dissociation of the dimer into two C_{60} fragments. (S_0 dissociates into two C_{60} singlets in their S_0 ground state, whereas T_1 and T_2 both fragment into one C_{60} singlet and one C_{60} triplet.)

The main features of the curves plotted in Figure 3 can be summarized as follows: (1) The S_0 and T_2 curves cross at distances shorter than that of the equilibrium configuration as expected.[11] (2) The S_0-T_2 crossings that these curves seem to present in the region of the S_0 barrier are merely an artifact of the comparison of synchronous and asynchronous curves and do not exist when one examines the curves plotted over the 3D PES. (3) In all states, dimer formation is predicted to be endothermic (E_F values in Table 1). (4) In the S_0 and T_1 states, the energy minimum is found at close values of both relevant inter- and intramolecular distances, which in turn are almost identical; the situation is different and less symmetric for the T_2 state. (5) The barriers towards dissociation differ remarkably.

A few comments about the above points are instructive: (i) The nature of the dimerization process is endothermic,[30] which is consistent with the fact that milder conditions (200 °C, normal pressure) are required for depolymerization to occur than for polymerization (800 K, 9 GPa).[31] (ii) The computed energy barriers for dissociation agree well with the available experimental data. (iii) The relative order between the states computed here differs from that obtained earlier using simple structural models[11] rather than the full-sized $C_{60}-C_{60}$ molecule.

From a physical point of view, the shape of the DFT curves in Figure 3 tends to confirm the validity of the mechanism proposed in ref 11 for the generation of magnetic moments, which does not require breaking the C_{60} cages. Indeed, they show that the application of pressure to pristine C_{60} induces a [2 + 2] cycloaddition reaction between adjacent C_{60} molecules to form a stable dimer (or higher oligomers, when more adjacent monomers are present) and suggest that for higher pressure a crossing between the S_0 and T_2 states may exist. However, the existence of the S_0-T_2 crossing still has to be proven; this requires the existence of a point on both the S_0 and T_2 curves that has the same energy at the same geometry.

The detailed analysis of the ethylene dimer surfaces as a function of the two interfragment C−C distances (within the 1.25−3.25 Å interval) revealed that no crossing existed along either a synchronous or an asynchronous pathway. Using these results as a guide, we also searched for such a crossing in the PES of the C_{60} dimer, but again we were unable to locate one. The next natural option was to explore the region in which one of the C_{60} fragments drifts laterally relative to the other. The corresponding rearrangement of the intermolecular interactions is shown in Figure 2. This reaction is expected to be endothermic and activated (because two C−C bonds are broken and just one is created). Note that the electronic structure of the singlet in this region is that of the diradical S_1. We computed the shape of the PES associated with the singlet and triplet T_2 states as a function of the interfragment C−C distance d and the drift δ. Our analysis identifies a crossing region and locates the lowest-energy crossing at $d = 1.503$ Å and $\delta = 1.45$ Å (d[6:6] = 1.570 Å), 75 kcal/mol above the S_0 ground-state energy.[32−34] Moreover, the drift motion along the S_0 PES from the minimum to the crossing point requires an energy barrier to be overcome, which we estimate to be 109 kcal/mol. Interestingly, both of these energy values are much smaller than that estimated from experiment for the loss of a C_2 unit from a C_{60} cage[35] and are also smaller than the estimated barrier (125 kcal/mol[36]) of a Stone-Wales rearrangement. Therefore, the creation of magnetic centers can take place at energies slightly below that needed for cage destruction and also below that associated with a competitive nondestructive process.

In summary, our investigation of the C_{60} dimers has confirmed and substantiated the basic steps of the mechanism proposed in ref 11 for the onset of ferromagnetic interactions in polymeric C_{60}. According to it, ferromagnetism can be induced when pressure is applied to the solid, and some of the $C_{60}-C_{60}$ units transform to a T_2-like configuration that remains stable once pressure is released. The probability that this magnetic state undergoes radiative decay is expected to be small because in the isolated $C_{60}-C_{60}$ dimers the transition from the T_2 minimum to the S_0 ground state is spin-forbidden as well as vibrationally forbidden.[11] Therefore, a scenario emerges in which the presence of a sufficient number of $C_{60}-C_{60}$ units in a T_2-like configuration combined with the existence of continuous ferromagnetic pathways accounts for the origin of macroscopic ferromagnetic properties. Our results also suggest new possible experimental procedures for the creation of ferromagnetic polymeric C_{60}. By irradiating a pristine C_{60} crystal, one could produce enough long-lived C_{60}(T) molecules that under pressure may undergo the reaction $C_{60}(T) + C_{60}(S) \rightarrow C_{60}-C_{60}(T_2)$, thus generating a sufficient number of $C_{60}-C_{60}$ units in T_2-like configurations. Under mild pressure conditions, the probability that units in T_1-like configurations are created is expected to be negligible because their formation barrier in the dimer is higher than that required for the formation of the T_2 state. However, the probability that ferromagnetic interactions are triggered by photochemical activation from the $C_{60}-C_{60}$ units in S_0-like conformations should be small because in the isolated dimer the S_0-T_2 transition is both spin- and vibrationally forbidden.[11]

Acknowledgment. J.J.N. thanks his colleagues at the IBM Zurich Research Laboratory for their kind hospitality. His visit there was made possible by a grant from the Department of Universities, Research, and Information Society of the Generalitat de Catalunya. J.J.N. also thanks the computing resources allocated by the CEPBA-IBM Research Institute, CEPBA, and CESCA to this work and the continuous financial support of the Spanish Ministerio de Ciencia y Tecnología (project BQU2002-04587-C02-02) and Comissionat per a Universitats i Recerca, Generalitat de Catalunya (grant 2001SGR-0044).

References and Notes

(1) Makarova, T. L.; Sundqvist, B.; Hohne, R.; Esquinazi, P.; Kopelevich, Y.; Scharff, P.; Davydov, V. A.; Kashevarova, L. S.; Rakhmanina, A. V. *Nature* **2001**, *413*, 716.

(2) Höhne, R.; Esquinazi, P. *Adv. Mater.* **2002**, *14*, 753.

(3) Wood, R. A.; Lewis, M. H.; Lees, M. R.; Bennington, S. M.; Cain, M. G.; Kitamura, N. *J. Phys.: Condens. Matter* **2002**, *14*, L385.

(4) Makarova, T. L.; Sundqvist, B.; Kopelevichm, Y. *Synth. Met.* **2003**, *137*, 1335.

(5) Narozhnyi, V. N.; Muller, K. H.; Eckert, D.; Teresiak, A.; Dunsch, L.; Davidov, V. A.; Kashevarova, L. S.; Rakhmanina, A. V. *Physica B* **2003**, *329*−*333*, 1217.

(6) Han, K. H.; Speman, D.; Höhne, R.; Setzer, A.; Makarova, T.; Esquinazi, P.; Buz, T. *Carbon* **2003**, *41*, 785.

(7) Wood, R. A.; Lewis, M. H.; Lees, M. R.; Bennington, S. M.; Cain, M. G.; Kitamura, N. *J. Phys.: Condens. Matter* **2002**, *14*, L385-L391.

(8) Andriotis, A. N.; Menon, M.; Sheetz, R. M.; Chernozatonskii, L. *Phys. Rev. Lett.* **2003**, *90*, 026801.

(9) Kim, Y. H.; Choi, J.; Chang, K. J.; Tomanek, D. *Phys. Rev. B* **2003**, *68*, 125420.

(10) Chan, J. A.; Montanari, B.; Gale, J. D.; Bennington, S. M.; Taylor, J. W.; Harrison, N. M. *Phys. Rev. B*, **2004**, *70*, 041403. This work reports on the existence of open-cage structures where new inter-C_{60} links are formed. No net magnetization was found for these open-cage systems. However, when H atoms are added in some parts of the cages, ferromagnetic interactions are detected.

(11) Ribas-Ariño, J.; Novoa, J. J. *Angew. Chem., Int. Ed. Engl.* **2004**, *43*, 577. Ribas-Ariño, J.; Novoa, J. J. *J. Phys. Chem. Solids* **2004**, *65*, 787.

(12) Belavin, V. V.; Bulusheva, L. G.; Okotrub, A. V.; Makarova, T. L. *Phys. Rev. B* **2004**, *70*, 155402.

(13) Parr, R. G.; Yang, W. *Density Functional Theory of Atoms and Molecules*; Oxford University Press: Oxford, U.K., 1994.

(14) For previous work on this dimer in the S_0 state, see, for example Xu, C. H.; Scuseria, G. E. *Phys. Rev. Lett.* **1995**, *74*, 274; Porezag, D.; Pederson, M. R.; Frauenheim, Th.; Köhler, Th. *Phys. Rev. B* **1995**, *52*, 14963; Kürti, J.; Németh, K. *Chem. Phys. Lett.* **1996**, *256*, 119; Osawa, S.; Sakai, M.; Osawa, E. *J. Phys. Chem. A* **1997**, *101*, 1378; Ozaki, T.; Iwasa, Y.; Mitani, T. *Chem. Phys. Lett.* **1998**, *285*, 289.

(15) *CPMD*, version 3.5.2, Copyright IBM Corporation 1990−2005, Copyright MPI für Festkörperforschung Stuttgart 1997−2001.

(16) Becke, A. D. *Phys. Rev. A* **1988**, *38*, 3098. Lee, C.; Yang, W.; Parr, R. G. *Phys. Rev. B* **1988**, *37*, 785.

(17) Troullier, N.; Martins, J. L. *Phys. Rev. B* **1991**, *43*, 1993.

(18) The $C_{60}-C_{60}$ dimer was placed in the center of an orthorhombic cell of dimensions (40; 24; 24) $(au)^3$.

(19) For a review, see Andreoni, W. *Annu. Rev. Phys. Chem.* **1998**, *49*, 405.

(20) Frisch, M. J.; Trucks, G. W.; Schlegel, H. B.; Scuseria, G. E.; Robb, M. A.; Cheeseman, J. R.; Zakrzewski, V. G.; Montgomery, J. A., Jr.; Stratmann, R. E.; Burant, J. C.; Dapprich, S.; Millam, J. M.; Daniels, A. D.; Kudin, K. N.; Strain, M. C.; Farkas, O.; Tomasi, J.; Barone, V.; Cossi, M.; Cammi, R.; Mennucci, B.; Pomelli, C.; Adamo, C.; Clifford, S.; Ochterski, J.; Petersson, G. A.; Ayala, P. Y.; Cui, Q.; Morokuma, K.; Malick, D. K.; Rabuck, A. D.; Raghavachari, K.; Foresman, J. B.; Cioslowski, J.; Ortiz, J. V.; Stefanov, B. B.; Liu, G.; Liashenko, A.; Piskorz, P.; Komaromi, I.; Gomperts, R.; Martin, R. L.; Fox, D. J.; Keith, T.; Al-Laham, M. A.; Peng, C. Y.; Nanayakkara, A.; Gonzalez, C.; Challacombe, M.; Gill, P. M. W.; Johnson, B. G.; Chen, W.; Wong, M. W.; Andres, J. L.; Head-Gordon, M.; Replogle, E. S.; Pople, J. A. *Gaussian 98*; Gaussian, Inc.: Pittsburgh, PA, 1998.

(21) Becke, A. D. *J. Chem. Phys.* **1993**, *98*, 5648.

(22) Noodlemann, L. *J. Chem. Phys.* **1981**, *74*, 5737. Noodlemann, L.; Davidson, E. R. *Chem. Phys.* **1986**, *109*, 131.

(23) (a) Bernandi, F.; Olivucci, M.; Robb, M. A. *Acc. Chem. Res.* **1990**, *23*, 405. (b) Bernardi, F.; Bottoni, A.; Olivucci, M.; Venturini, A.; Robb, M. A. *J. Chem. Soc., Faraday Trans.* **1994**, *90*, 1617.

(24) Similar agreement between the broken-symmetry and CASSCF potential energy surfaces have already been reported in the literature. See, for instance, Goldstein, E.; Beno, B.; Houk, K. N. *J. Am. Chem. Soc.* **1996**, *118*, 6036.

(25) Nuñez-Regueiro, M.; Monceau, P.; Rassat, A.; Bernier, P.; Zahab, A. *Nature* **1991**, *354*, 289. Rao, A. M.; Zhou, P.; Wang, K. A.; Hager, G. T.; Holden, J. M.; Wang, Y.; Lee, W. T.; Bi, X.-X.; Eklund, P. C.; Cornett, D. S.; Duncan, M. A.; Amster, I. J. *Science* **1993**, *259*, 955.

(26) Wang, G.-W.; Komatsu, K.; Murata, Y.; Shiro, M. *Nature* **1997**, *387*, 583.

(27) Nuñez-Regueiro, M.; Marques, L.; Hodeau, J.-L.; Béthoux, O.; Perroux, M. *Phys. Rev. Lett.* **1995**, *74*, 278.

(28) (a) Bachilo, S. M.; Benedetto, A. F.; Weisman, R. B. *J. Phys. Chem. A* **2001**, *105*, 9845. (b) Yamaguchi, S.; Funayama, T.; Ohba, Y.; Paul, P.; Reed, C. A.; Fujiwara, K.; Komatsu, K. *Chem. Phys, Lett.* **2002**, *363*, 199.

(29) Wasielevski, M. R.; O'Neil, M. P.; Lykke, K. R.; Pellin, M. J.; Gruen, D. M. *J. Am. Chem. Soc.* **1991**, *113*, 2772.

(30) Previous B3LYP/3-21G calculations (Scuseria, G. E. *Chem. Phys. Lett.* **1996**, *257*, 583) pointed to the instability of the dimer. However, we found that this is an artifact due to the use of small Gaussian basis sets, which can be corrected using larger basis sets (e.g., at the B3LYP/6-31G-(d) level E_F is 2.6 kcal/mol).

(31) Makarova, T. L. *Semiconductors* **2001**, *35*, 257.

(32) In the Landau−Zener model, the S_0-T_2 crossing probability is proportional to the spin−orbit coupling matrix element between the S_0 and T_2 states, the velocity of the system in the crossing region, and the difference between the gradients of the S_0 and T_2 potential energy curves in that crossing point. We have computed the spin−orbit coupling matrix element in the S_0-T_2 crossing point for the ethene dimer and a $C_{18}H_{12}$ dimer built from the C_{60} dimer by selecting all C═C units that constitute the 6:6 bond involved in this dimer [2 + 2] cycloaddition, its fused six-membered rings, and the two five-membered rings attached to them (the external C═C units were also included in the model). Hydrogen atoms were attached to the broken C−C bonds to saturate them. At the CAS(6,6)/3-21G level, the S_0-T_2 spin−orbit couplings for these two dimers were estimated to be 0.33 and 0.16 cm^{-1}, respectively, which are small but nonnegligible values. The procedure outlined in ref 33, as implemented in GAMESS (ref 34), was employed.

(33) Matsunaga, N.; Koseki, S.; Gordon, M. S. *J. Chem. Phys.* **1996**, *104*, 7988.

(34) Schmidt, M. W.; Baldridge, K. K.; Boatz, J. A.; Elbert, S. T.; Gordon, M. S.; Jensen, J. H.; Koseki, S.; Matsunaga, N.; Nguyen, K. A.; Su, S. J.; Windus, T. L.; Dupuis, M.; Montgomery, J. A. *J. Comput. Chem.* **1993**, *14*, 1347.

(35) Wurz, P.; Lykke, K. R. *Chem. Phys.* **1994**, *184*, 335.

(36) Yi, J.-Y.; Bernholc, J. *J. Chem. Phys.* **1992**, *96*, 8634.